

Comparison of Layerwise Preheating and Post-heating Laser Scan on The Microstructure and Mechanical Properties of L-PBF Ti6Al4V

Ahmet Alptug Tanrikulu^{1,2}, Aditya Ganesh-Ram³, Behzad Farhang³, Amirhesam Amerinatanzi^{1,3}

¹ Materials Science and Engineering, University of Texas at Arlington, Arlington, TX, USA

² Turkish Aerospace Industries, Ankara, Turkey

³ Mechanical and Aerospace Engineering, University of Texas at Arlington, Arlington, TX, USA

Abstract

This study aimed to investigate the evolution of the microstructure and mechanical properties of as-fabricated laser powder bed fusion (L-PBF) Ti-6Al-4V samples by introducing layerwise pre-heating or post-heating laser scans. Multiple laser scans, varying in scanning speed at constant power, were examined before the melting laser scan (pre-heating) or after it (post-heating). The analysis focused on microstructural features such as porosity, and α -phases lath structure, as well as the hardness response of the material. The results revealed the additional layerwise scans had a significant impact on reducing porosity by up to 98% when the additional scan was applied prior to or upon the melting scan. Additional laser scans decreased the microstructure and mechanical response variation along different orientations. Furthermore, these findings highlight the potential of layerwise heating strategies to improve the overall quality and performance of L-PBF Ti-6Al-4V components, thus paving the way for enhanced applications in various industries such as aerospace.

Keywords: Laser powder bed fusion, Ti6Al4V, Preheating Scan, Post-heating Scan, Microstructure

1. Introduction

Ti6Al4V material is one of the most preferred titanium alloys renowned for its outstanding mechanical properties [1]. Its remarkable strength-to-weight ratio, extraordinary fracture toughness, resistance at corrosive environments, and biocompatibility have made it an approved choice for manufacturing durable lightweight components needed for the automotive, aerospace, and biomedical industries [2]. These exceptional aspects have gained Ti6Al4V significant popularity for additive manufacturing (AM) applications [2].

AM technology was invented in the 1980s and emerged as a revolutionary process of joining materials layer upon layer to fabricate parts directly from the digital 3D file of the geometry. This technique has shown rapid development due to the superior fabrication ability of complex geometries compared to traditional fabrication techniques. Additionally, the near-net-shape production capability of AM technology enhanced the sustainability of the fabrication by reducing material waste and energy needs required for conventional manufacturing. With the advancement of novel free-form design approaches by topology optimization, AM technology continues to gain momentum by eliminating the design limitations of traditional fabrication methods [3]. Laser powder bed fusion (LPBF) is the most adequate technique for these ingenious design approaches among all the other AM technologies due to its ability to fabricate fine features with high resolution [4].

Utilizing the capabilities of the LPBF techniques on Ti6Al4V material allows the fabrication of complex-shaped lightweight engineering parts with exceptional mechanical properties. However, its remarkable properties, due to the rapid solidification and cooling rates during the LPBF process

microstructure of Ti6Al4V material have challenges to be addressed. Additionally, heat dissipation differences between the building direction and building plane make the Ti6Al4V microstructure more complicated. In the LPBF process when the laser heat source interacts with the metal powder melting and solidification occurred in a very confined region with a very rapid time manner. After the laser scan, a substantial amount of heat dissipates through the material underneath the melt pool, resulting in a directional grain growth during the solidification. Thus, the microstructure of Ti6Al4V processed by LPBF technology has non-uniform grain structure. The microstructure variation is the fundamental source of the anisotropic mechanical behavior of the LPBFed Ti6Al4V material which is one of the most frequently studied properties of the material [5]. A great number of reported studies were seeking a solution to address this issue through the application of post-heat treatment (HT) [6] which requires additional research effort to optimize the effect on microstructure. The application of HT increases the production cost with the necessity to advance equipment such as a hot isostatic pressure (HIP) furnace or controlled environment HT furnace. To avoid the additional cost of HT on LPBFed Ti6Al4V material, preheating laser scan, and post-heating laser scan studies were proposed to improve microstructure uniformity by controlling the heat input and cooling rates during the fabrication.

In this study, the proposed innovative solutions of preheating laser scan and post-heating laser scan applications during the LPBF fabrication were evaluated. An additional laser scan was applied with a variety of laser scan speeds prior to the melting scan for preheating while a sequent laser scan was applied at a variety of scan speeds upon the melting scan to regulate the directional grain growth. Results showed that both applications had a significant effect on the microstructure and mechanical response of the material and their effects were evaluated and compared in the presented study.

2. Materials and Methods

The material used in this study was gas-atomized Ti6Al4V Grade 5 powder, supplied by EOS North America (Pflugerville, TX, USA). The chemical composition(wt.%) of the powder consisted of 5.50 - 6.75 Al, 3.50 - 4.50 V, 0.20 O, 0.05 N, 0.08 C, 0.015 H, 0.30 Fe, and balance Ti, in accordance with ISO 5832-3, ASTM F1472, ASTM F2924, and ASTM F3302 standards. The powder has a particle size distribution from 20 μm to 80 μm [7].

The samples with a rectangular prism shape (Figure 1) were fabricated by LPBF technology on an EOS M290 SLM printer (EOS GmbH, Electro Optical Systems, Krailling, Germany) with a capacity of 400W Yb: YAG fiber laser. The building plate was preheated to 80°C to reduce the thermal gradient at the initial layers of the fabrication.

In this study, the effect of the innovative approaches of layerwise preheating and post-heating laser scan applications on the Ti6Al4V material's microstructure and mechanical behavior was compared and discussed in detail. In both applications, the powder material was exposed to laser scan twice. Only the reference sample was exposed to a single laser track with the default process parameters of the LPBF process which were 280W laser power, 1300mm/s laser scan speed, 40 μm layer thickness, 67° scan rotation, 100 μm laser spot diameter and 100 μm hatch spacing.

For preheating application, samples were exposed to a laser scan prior to the melting scan of default parameters whereas post-heating samples were exposed to a laser scan upon the melting laser scan. For both applications, the effect of five different laser scan speeds at constant laser power with a total of five variations each was evaluated.

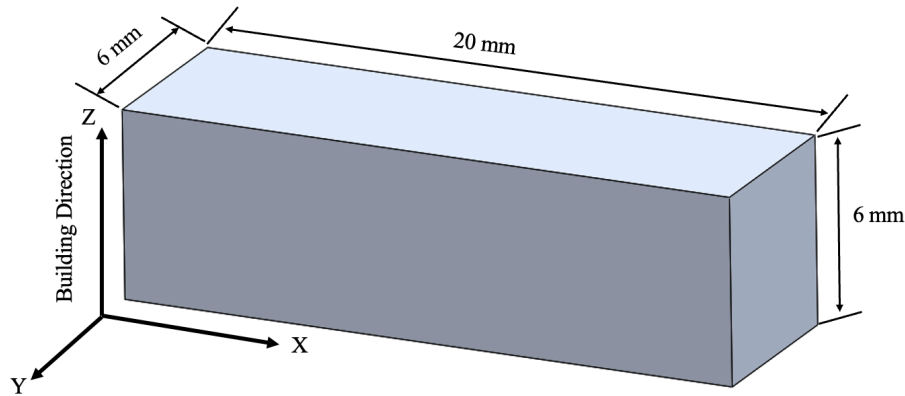


Figure 1. Schematic view and the orientation of the rectangular prism shape samples. The cartesian coordinates show the building direction along the Z-axis. The microstructural evaluation and mechanical testing were conducted along the ZX plane and XY plane to distinguish the effect of the orientation on microstructure and mechanical properties.

Microstructure characterization was conducted to reveal the microstructure properties of porosity and α -phase lath thickness. A HITACHI S-3000N Variable Pressure Scanning Electron Microscopy (SEM) was used for microstructure imaging. Samples were cold-mounted before grinding and polishing. E-prep 4TM automated polisher was used for grinding (320 to 1200 Grit size silicon carbide abrasive discs) and polishing (1 μm diamond suspension on DiaMat polishing cloth and 0.04 μm colloidal silica for final polishing on a Chem-pol polishing cloth) with an individual force and rotation speed of the power head. The samples were cleaned with micro-organic soap and rinsed with isopropyl alcohol. The samples were etched before microstructure characterization by Kroll's reagent (1-3 mL, HF, 2-6 mL HNO₃, 100 mL water) to depict the lath structure and grain boundaries.

An image analysis software Image J [8], was employed to quantize the porosity percentage and the thickness of the α -phase laths. The porosity level of the microstructure was evaluated in at least three regions of two magnification levels (500x and 800x). For lath thickness measurement microstructure images were first converted to RGB stack-type grayscale images prior to adjusting the contrast level. Then the threshold was adjusted by utilizing the auto-threshold comment of the software to create distinct contrast between individual laths. Particle analysis was employed between the range from 0.2 μm to 2.0 μm and the total particle counts were summarized for the mean value. This calculation was performed on at least six images at different magnification levels between 800x to 1500x for both XY and ZX planes.

LECO LM 300 AT Micro Hardness tester equipment was used for the microhardness test, 500 g load was applied for 10 seconds in accordance with ASTM E384-22 [9]. Samples were polished including the final polishing step with 0.04 μm colloidal silica before the hardness test and at least 12 indentations were conducted for each sample.

3. Results and Discussions

3.1 Microstructural Analysis

3.1.1 Porosity

The porosity levels of each sample were calculated by processing the SEM micrographs from at least three different regions that were captured at the magnification levels mentioned in Section 2. The porosity level of the reference sample without any preheating or post-heating laser scan was observed at $0.47\% \pm 0.015$ and depicted with a black triangle marker in Figure 2.

A remarkable improvement in the LPBF Ti6Al4V material's relative density was observed with the application of each preheating and post-heating laser scan. The authors observed the lowest porosity values at the defined laser power values of 252 W and 140 W for preheating and post-heating applications relatively. The effect of the primary laser scan speed, during the preheating process, on porosity is shown in black (Fig. 2). All the preheating applications were conducted at a constant laser power of 252 W, and apart from the scan speed, all the process parameters were set to the default parameters mentioned in Section 2. The porosity results of the preheating laser scan speed of 650 mm/s, 975 mm/s, 1300 mm/s, 1625 mm/s, and 1950 mm/s were calculated. It was observed that the additional laser scan prior to the melting scan decreased the porosity level up to 0.01 %.

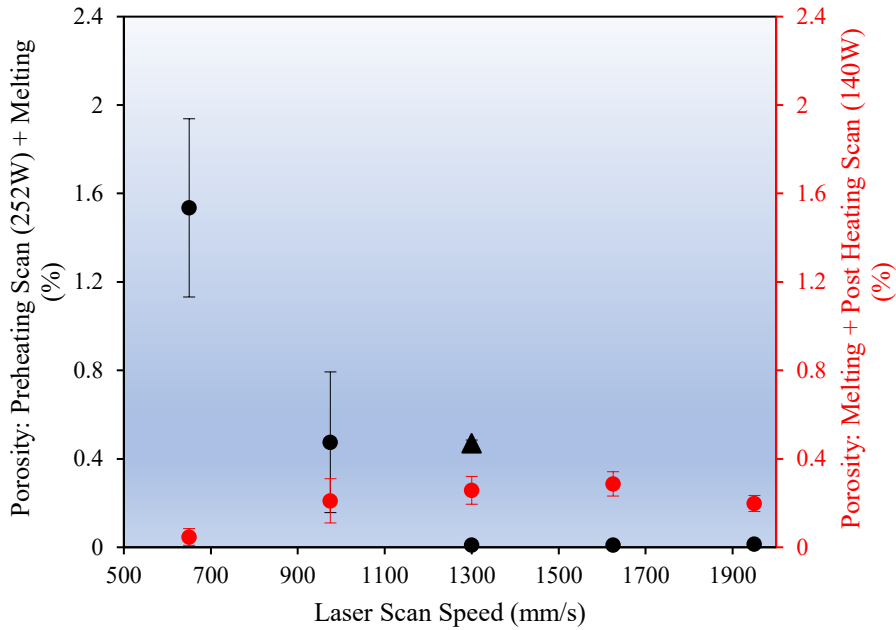


Figure 2. The effect of the preheating laser scan speed on porosity at a constant preheating laser power of 252 W (in black) and the effect of the post-heating laser scan speed on the porosity at a constant post-heating laser power of 140 W (in red).

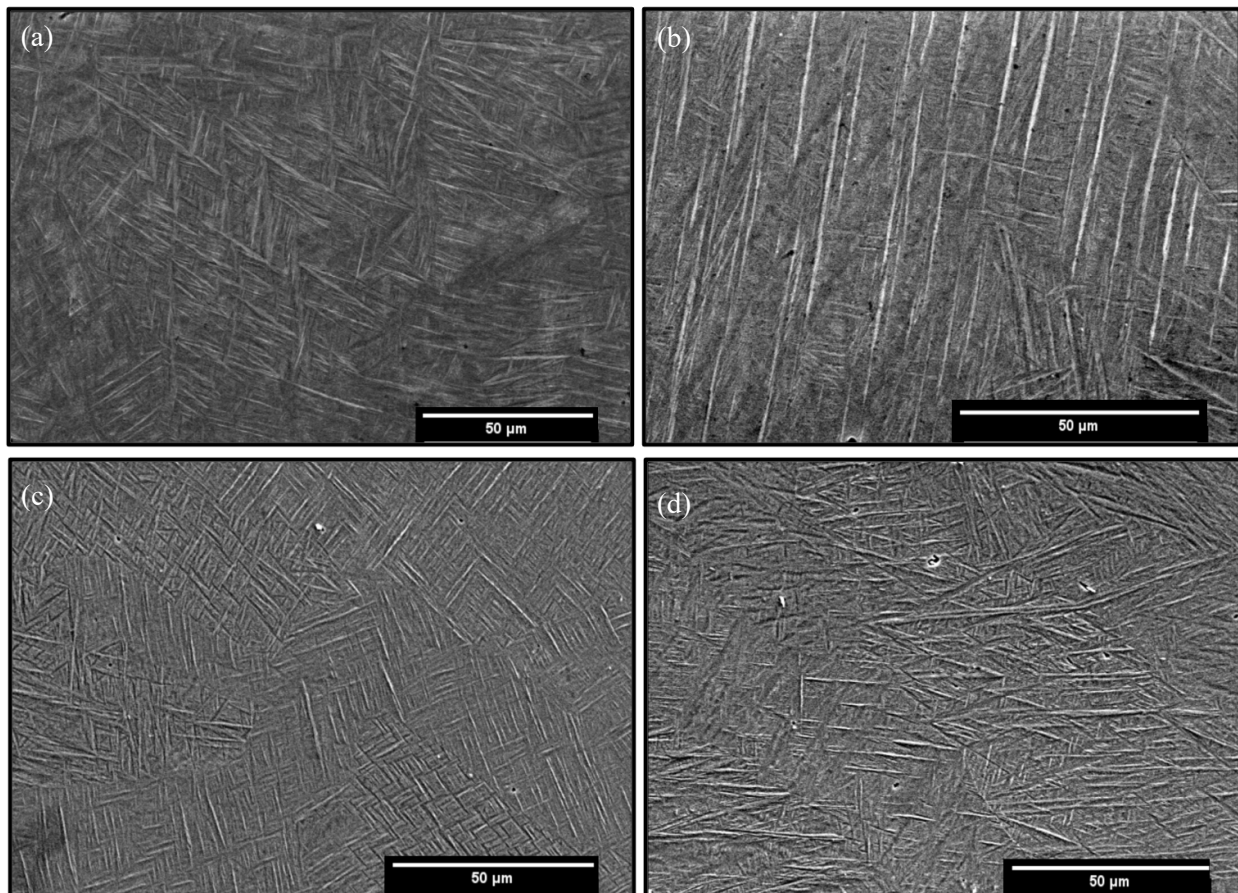
A decremental trend in porosity level was observed in the case of preheating applications with higher preheating laser scan speeds at lower energy inputs resulting in a lower amount of porosity. An excessive porosity amount was observed at the preheating laser scan speed of 650 mm/s. The energy density of this preheating laser scan speed was 80.77 J/mm^3 which was 1.8 times higher than the manufacturer's optimized melting energy density (44.87 J/mm^3). This redundant heat input formed an unstable melt pool with a higher amount of metal evaporation which increased the recoil pressure. Unbalanced recoil pressure provoked molten metal expulsion as spatters [10]. A higher amount of spattering at the excessive energy input level contributed to a higher porosity level [11] in the microstructure of the preheated sample. Contrary to the lower scan speed rate, almost porosity-free microstructures (relative density $\sim 99.99\%$) were obtained at the higher preheating laser scan speeds of 1300 mm/s, 1625 mm/s, and 1950 mm/s.

Similar to the preheating application, process parameters were kept identical to the default parameters except for the laser power and laser scan speed during the post-heating scan upon the melting laser scan. It was observed that the inherent porosity level of the microstructure decreased with the application of the post-heating laser scan for each scanning speed. The lowest porosity amount was observed at the post-heating scan speed of 650 mm/s with a percentage of $0.047\% \pm 0.038$. However, the improvement in porosity was limited in post-heating application compared to preheating, it was still 50% less than the initial microstructure of the reference sample.

The process-induced inherent porosities have a detrimental effect on the mechanical properties of LPBFed Ti6Al4V materials [12]. It is known that a complementary process of hot isostatic pressure (HIP) was applied to as-build LPBF Ti6Al4V to improve the porosity level of the microstructure [13]. In this study, a similar improvement in the porosity level delivered by HIP post-process was observed for both preheating-laser-scanned and post-heating-laser-scanned Ti6Al4V microstructure. This can be considered as a promise by the application of additional laser scans as an alternate procedure for the expensive and time-consuming post-process of HIP to decrease the inherent porosity level of the LPBFed Ti6Al4V microstructure. Additionally, this promise of the proposed applications has the potential of superior mechanical properties of elongation [14] and fatigue strength [15] with lower process-induced defects.

3.1.2 Grain Structure

The $\alpha + \beta$ titanium alloy Ti6Al4V microstructure was characterized and it was detected that the majority of the LPBFed material's microstructure consisted of α -phase at room temperature. As the dominant phase, it is rational to evaluate the α -phase properties to correlate the microstructure and the mechanical response of the material. α -phase has a basketweave-like grain structure in which the lath thickness contributes to the material's properties [16]. Figure 3 shows the lath structure of the samples along the XY and ZX planes for reference samples ((a) and (b)), preheating laser scan application samples ((c) and (d)), and post-heating laser scan application samples ((e) and (f)).



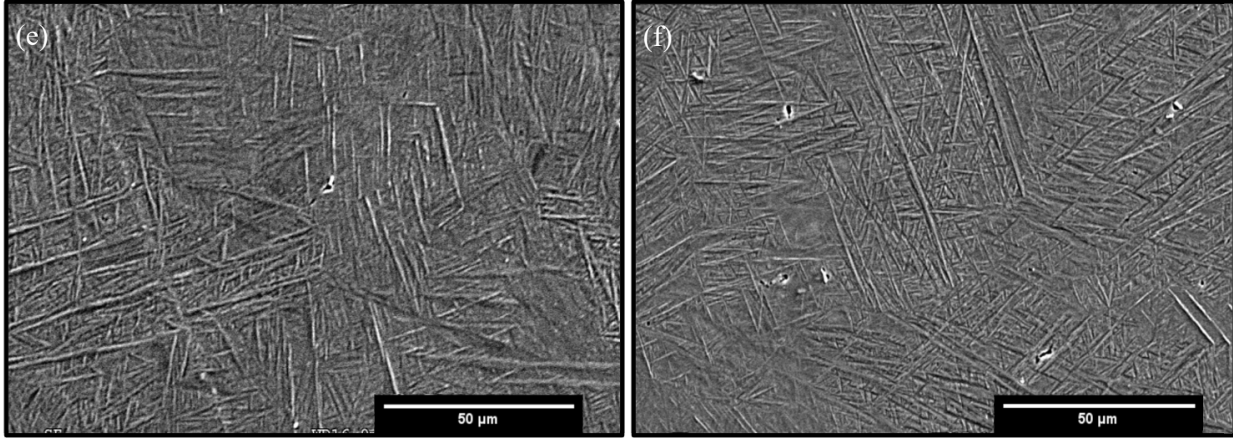


Figure 3. SEM microstructure of the reference sample along the XY plane (a), along the ZX plane (b), Microstructure of the preheating laser scan application at 252W laser power and 1950 mm/s scan speed along the XY plane (c), and along the ZX plane (d), Microstructure of the post-heating laser scan application at 140W laser power and 1950 mm/s scan speed along the XY plane (e) and along the ZX plane (f).

The variety in the microstructure of the reference Ti6Al4V between the XY and ZX planes was because of the directional solidification that occurred during the fabrication. Since a significant amount of heat is dissipated through the fabricated material underneath the melt pool, the cooling rate along the building direction (z-axis) was higher compared to the other axes. Thus, the microstructure along the different axes had different grain morphology. In the presented study, this nonuniformity of the microstructure along the different orientations was investigated by analyzing the constituent α -phase lath structures. Figure 4 shows the effect of the preheating and post-heating laser scan on α -phase lath thickness. It was observed that the applied preheating and post-heating laser scans modified the microstructure and decreased the thickness variation among different orientations.

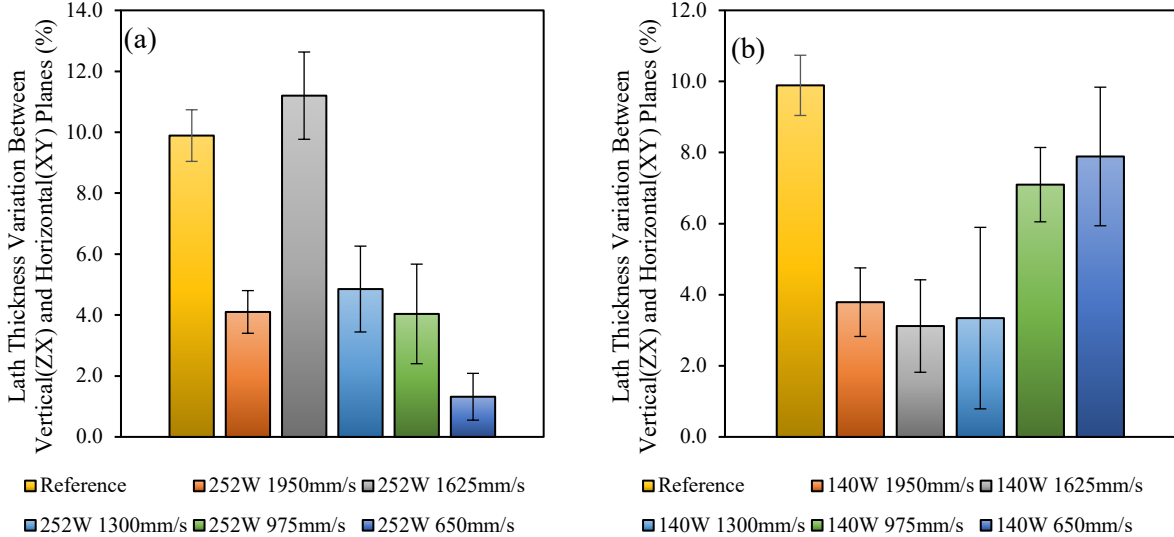


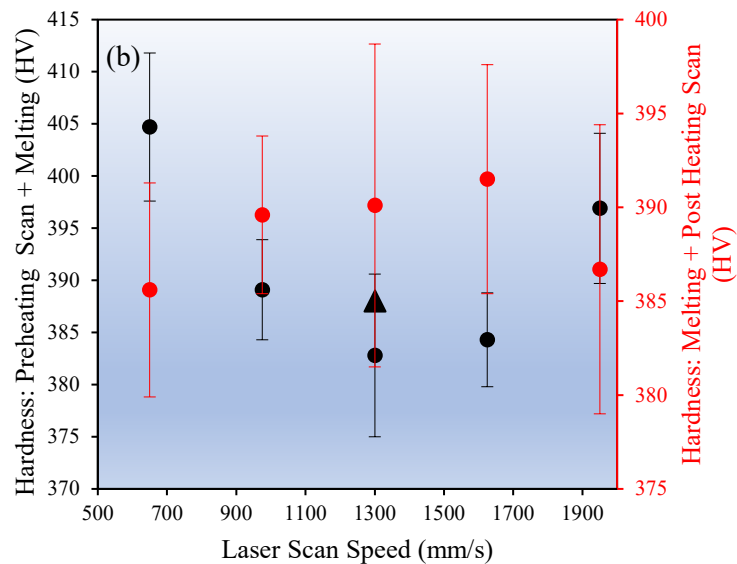
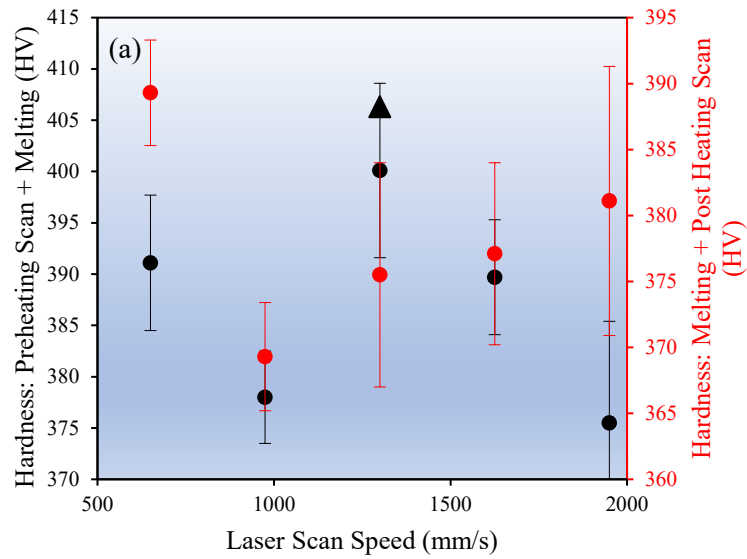
Figure 4. (a) The effect of the preheating laser scans on the α -phase lath thickness variation between the XY and ZX planes. (b) The effect of the post-heating laser scans on the α -phase lath thickness variation between the XY and ZX planes.

The non-uniform microstructure of the LPBFed Ti6Al4V is the fundamental reason for the anisotropic mechanical response of this material. The anisotropic mechanical properties are still a challenge that needs

to be addressed to utilize this technology further in industrial engineering applications. Previous studies [12,17] reported modifications in α -phase lath structure by employing post-heat treatments which required additional technical effort and cost to optimize the heat treatment process. The techniques in this study contributed to lath structure modification which resulted in lesser variation among the different orientations. This was considered as the proven result of the preheating and post-heating laser scan applications on the improved isotropy of the LPBFed Ti6Al4V microstructure and mechanical properties.

3.2 Mechanical Testing

Microhardness tests were conducted to analyze the effect of preheating and post-heating laser scans on the mechanical behavior of LPBFed Ti6Al4V. The reference sample's hardness was measured as 406.3 ± 4.6 HV and 388 ± 4.4 HV along the XY and ZX planes respectively. Figures 5 (a) and (b) show the measured hardness values of the preheating and post-heating samples at different laser scan speeds. The reference sample without any preheating or post-heating laser scan was shown with a black triangle marker.



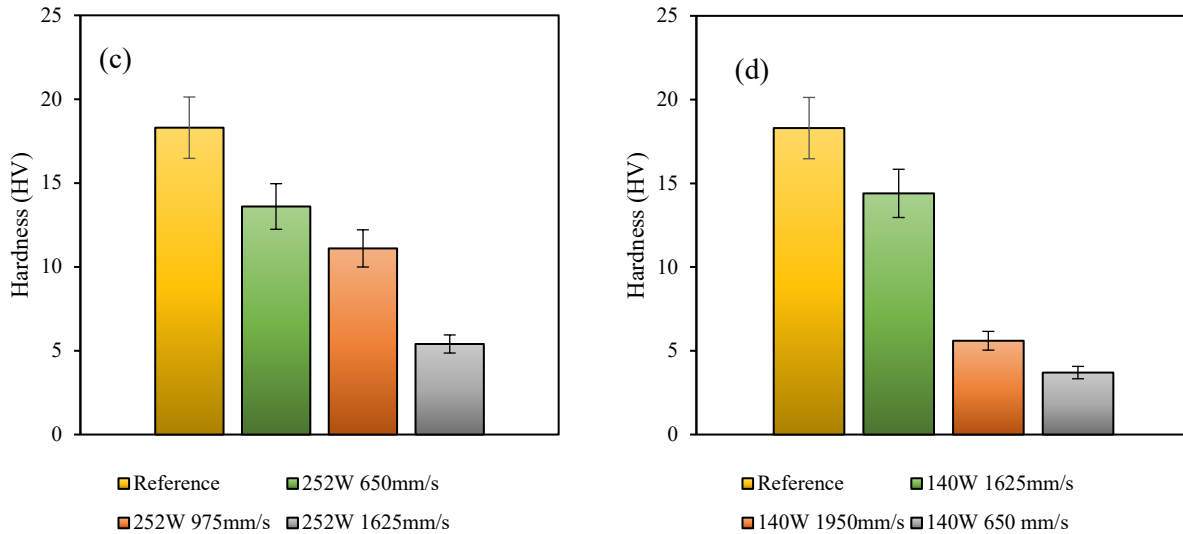


Figure 5. (a) The effect of the laser scan speed on the microhardness of the LPBFed Ti6Al4V during preheating and post-heating laser scan along the XY plane. (b) The effect of the laser scan speed on the microhardness of the LPBFed Ti6Al4V during preheating and post-heating laser scan along the ZX plane. (c) Hardness difference between XY and ZX planes after the application of preheating laser scan speed at different scan speeds. (d) Hardness difference between XY and ZX planes after the application of post-heating laser scan speed at different scan speeds.

It was observed that preheating laser scan speed has a significant effect on the hardness along the XY plane. The highest degradation in hardness was observed at the preheating laser scan of 1950 mm/s. The microstructure response after the preheating laser scan to the hardness along the ZX plane was not similar to the response along the XY plane. Although hardness decreased at the preheating laser scan speed of 1300 mm/s and 1625 mm/s, vice versa was found at the other scan speeds. The highest hardness improvement along the ZX plane with the preheating laser scan application was observed at the scan speed of 650 mm/s and the lowest degradation was observed at the scan speed of 1300 mm/s.

Increasing post-heating laser scan speed from 975 mm/s to 1950 mm/s, the hardness of the LPBFed Ti6Al4V microstructure was increased compared to the reference condition along the XY plane. The highest degradation of hardness was observed at the scan speed of 975 mm/s. The hardness change after applying the post-heating laser scan along the ZX plane was not similar to the change on the XY plane. Contrary to the response along the XY plane slight changes (<1%) in hardness were observed along the ZX plane after the application of the post-heating laser scan.

Figures 5 (c) and (d) show that the application of preheating and post-heating laser scans decreased the hardness variation of the LPBFed Ti6Al4V microstructure between the XY and ZX planes at the reference condition. This observation was in parallel with the results discovered during the microstructure evaluation of the α -phase lath structures.

In this study, it was observed that the challenge of the anisotropic mechanical response due to the non-uniform microstructure of LPBFed Ti6Al4V can be addressed with additional laser scans prior to, or upon the melting scan of the process. This promise of the compared applications has the potential to skip the heat treatments applied after the fabrication. The effect of the compared applications on other microstructure features and mechanical properties of the LPBFed Ti6Al4V will be investigated by the authors in future studies.

4. Conclusion

In this study, the effect of the preheating laser scan and post-heating laser scan on LPBFed Ti6Al4V material's microstructure was observed. The mechanical response also have been evaluated through hardness measurements and it has been concluded that post-heat treatment processes need not be required if they are used during fabrication. The findings of this study listed as:

- Preheating laser scan application prior to the melting scan with the default parameters had a significant effect on the inherent porosity level of the LPBFed Ti6Al4V material. It was observed that preheating scan application decreased the porosity level of the reference condition from 0.47% to 0.01%.
- Application of the preheating scan modified the microstructure by decreasing the α -phase lath thickness variation between XY and ZX planes and created a more uniform grain structure along different orientation. It was observed that the variation decreased to 1.3% between the planes.
- Preheating laser scan application has a significant effect on the hardness values of the material. It was observed that the hardness variation between the XY and ZX planes decreased by less than 1.5%.
- Post-heating laser scan application upon the melting scan had a similar effect on the process-induced inherent porosity level as the preheating application. Compared to the preheating, post-heating scan had a limited effect on porosity but it was still 50% less than the reference condition of the LPBFed Ti6Al4V material.
- Post-heating laser scan application improved the uniformity of the Ti6Al4V microstructure by decreasing the α -phase lath thickness variation between the XY and ZX planes. It was observed that the variation decreased to 3.1% between the planes which was not as significant as the preheating application.
- Post-heating laser scan decreased the anisotropic mechanical response by decreasing the variation of the hardness between the XY and ZX planes up to 3.7% for LPBF-processed Ti6Al4V material.

5. References

- [1] S. Liu, Y.C. Shin, Additive manufacturing of Ti6Al4V alloy: A review, *Mater Des.* 164 (2019) 107552. <https://doi.org/https://doi.org/10.1016/j.matdes.2018.107552>.
- [2] T.S. Tshephe, S.O. Akinwamide, E. Olevsky, P.A. Olubambi, Additive manufacturing of titanium-based alloys- A review of methods, properties, challenges, and prospects, *Heliyon.* 8 (2022) e09041. <https://doi.org/https://doi.org/10.1016/j.heliyon.2022.e09041>.
- [3] A.M. Vilardeell, A. Takezawa, A. du Plessis, N. Takata, P. Krakhmalev, M. Kobashi, I. Yadroitsava, I. Yadroitsev, Topology optimization and characterization of Ti6Al4V ELI cellular lattice structures by laser powder bed fusion for biomedical applications, *Materials Science and Engineering: A.* 766 (2019) 138330. <https://doi.org/10.1016/j.msea.2019.138330>.
- [4] Z. Wu, S.P. Narra, A. Rollett, Exploring the fabrication limits of thin-wall structures in a laser powder bed fusion process, *The International Journal of Advanced Manufacturing Technology.* 110 (2020) 191–207. <https://doi.org/10.1007/s00170-020-05827-4>.
- [5] M.-W. Wu, K. Ni, H.-W. Yen, J.-K. Chen, P. Wang, Y.-J. Tseng, M.-K. Tsai, S.-H. Wang, P.-H. Lai, M.-H. Ku, Revealing the intensified preferred orientation and factors dominating the anisotropic mechanical properties of laser powder bed fusion Ti-6Al-4V alloy after heat treatment, *J Alloys Compd.* 949 (2023) 169494. <https://doi.org/10.1016/j.jallcom.2023.169494>.
- [6] F. Bartolomeu, M. Gasik, F.S. Silva, G. Miranda, Mechanical Properties of Ti6Al4V Fabricated by Laser Powder Bed Fusion: A Review Focused on the Processing and Microstructural Parameters Influence on the Final Properties, *Metals (Basel).* 12 (2022) 986. <https://doi.org/10.3390/met12060986>.

- [7] EOS GmbH, EOS Titanium Ti64 - Material data sheet, (2017). <https://www.eos.info/material-m>.
- [8] C.A. Schneider, W.S. Rasband, K.W. Eliceiri, NIH Image to ImageJ: 25 years of image analysis, *Nat Methods*. 9 (2012) 671–675. <https://doi.org/10.1038/nmeth.2089>.
- [9] Standard Test Method for Microindentation Hardness of Materials 1, (n.d.). <https://doi.org/10.1520/E0384-22>.
- [10] A. Ganesh-Ram, M. Hanumantha, B.B. Ravichander, B. Farhang, S. Ramachandra, N.S. Moghaddam, A. Amerinatanzi, STUDY OF SPATTER FORMATION AND EFFECT OF ANTI-SPATTER LIQUID IN LASER POWDER BED FUSION PROCESSED Ti-6Al-4V SAMPLES, n.d.
- [11] D. Wang, S. Wu, F. Fu, S. Mai, Y. Yang, Y. Liu, C. Song, Mechanisms and characteristics of spatter generation in SLM processing and its effect on the properties, *Mater Des*. 117 (2017) 121–130. <https://doi.org/10.1016/j.matdes.2016.12.060>.
- [12] S. Cao, Y. Zou, C.V.S. Lim, X. Wu, Review of laser powder bed fusion (LPBF) fabricated Ti-6Al-4V: process, post-process treatment, microstructure, and property, *Light: Advanced Manufacturing*. 2 (2021) 1. <https://doi.org/10.37188/lam.2021.020>.
- [13] A. du Plessis, E. Macdonald, Hot isostatic pressing in metal additive manufacturing: X-ray tomography reveals details of pore closure, *Addit Manuf*. 34 (2020) 101191. <https://doi.org/10.1016/j.addma.2020.101191>.
- [14] C. Qiu, N.J.E. Adkins, M.M. Attallah, Microstructure and tensile properties of selectively laser-melted and of HIPed laser-melted Ti-6Al-4V, *Materials Science and Engineering: A*. 578 (2013) 230–239. <https://doi.org/10.1016/j.msea.2013.04.099>.
- [15] S. Leuders, M. Thöne, A. Riemer, T. Niendorf, T. Tröster, H.A. Richard, H.J. Maier, On the mechanical behaviour of titanium alloy TiAl6V4 manufactured by selective laser melting: Fatigue resistance and crack growth performance, *Int J Fatigue*. 48 (2013) 300–307. <https://doi.org/10.1016/j.ijfatigue.2012.11.011>.
- [16] X. Du, M. Simonelli, J.W. Murray, A.T. Clare, Facile manipulation of mechanical properties of Ti-6Al-4V through composition tailoring in laser powder bed fusion, *J Alloys Compd*. 941 (2023) 169022. <https://doi.org/10.1016/j.jallcom.2023.169022>.
- [17] S.A. Etesami, B. Fotovvati, E. Asadi, Heat treatment of Ti-6Al-4V alloy manufactured by laser-based powder-bed fusion: Process, microstructures, and mechanical properties correlations, *J Alloys Compd*. 895 (2022) 162618. <https://doi.org/10.1016/j.jallcom.2021.162618>.